AIAA JOURNAL
Vol. 33, No. 9, September 1995

Perpendicular Blade Vortex Interaction

Kenneth S. Wittmer,* William J. Devenport,† and Michael C. Rife‡
Virginia Polytechnic Institute and State University, Blacksburg, Virginia 24061
and
Stewart A. L. Glegg§
Florida Atlantic University, Boca Raton, Florida 33431

The interaction between a streamwise vortex and a spanwise blade was studied in incompressible flow for blade-vortex separations between ±1/8 chord. Three-component velocity and turbulence measurements were made from 4 chord lengths upstream to 15 chord lengths downstream of the blade using miniature four-sensor hot-wire probes. The interaction of the vortex with the blade causes an almost immediate loss in vortex core circulation. Downstream of the blade the core becomes embedded in the blade wake and begins to grow rapidly. Core radius increases and peak tangential velocity decreases but circulation remains roughly constant. True turbulence levels within the core are much larger downstream than upstream of the blade. Outside of the core the interaction produces a substantial region of turbulent flow associated with the blade and vortex generator wakes. Overall, perpendicular blade vortex interaction substantially alters the flow and produces a much larger and more intense region of turbulent flow than that presented by the undisturbed vortex. These results have significant implications for the prediction of both impulsive and broadband helicopter noise.

Nomenclature

c	= vortex generator and interaction blade chord length, 0.203 m
f	= frequency, 1/s
G_{uu}, G_{vv}, G_{ww}	= u, v,and w velocity autospectra, respectively, m²/s
k	= turbulent kinetic energy, m²/s²
r_1	= vortex core radius measured from the core center to the point of peak tangential velocity, m
U, V, W	= mean velocities in the x, y, and z directions, respectively, m/s
U_{ref}	= freestream reference velocity, m/s
U_0	= axial velocity in the vortex core center, m/s
u, v, w	= fluctuating velocities in the x, y, and z, directions, respectively, m/s
$V_{\theta 1}$	= peak tangential velocity in vortex core, m/s
x, y, z	= coordinates defined in Fig. 2, m
z_0	= z location of the generator vortex center, m
α	= angle of attack of the blade, positive about negative y axis, as shown in Fig. 2
Δ	= blade-vortex separation distance defined in Fig. 2, m
Γ_0	= root circulation of the vortex generator calculated using lifting line theory, m²/s
Γ_1	= vortex core circulation defined as $2\pi r_1 V_{\theta 1}$, m²/s
ω_x	= mean axial vorticity, 1/s

Introduction

BLADE vortex interactions (BVI) in helicopter rotors generate substantial acoustic noise. Parallel interactions (causing impulsive BVI noise) have been the subject of many previous studies in both fluid mechanics and acoustics. Perpendicular interactions [causing broadband blade-wake interaction (BWI) noise] have received relatively little attention and are not well understood, even though they are an important contributor to helicopter noise during level flight and mild climb conditions.[1]

The objective of the work described here is to improve understanding of perpendicular interactions, specifically, the effects of such interactions on the vortex, and to use this new information to improve noise predictions. The effects on the vortex are of interest because it is common in helicopter rotor flows for several blades to interact with the same vortex. If the first interaction significantly alters the vortex core, then all subsequent interactions will be affected, modifying the whole rotor-plane flow and presumably the noise it generates. This suggestion is indirectly supported by the work of Devenport et al.,[2] who studied the turbulence and spectral structure of an undisturbed trailing vortex and incorporated the data into the BWI noise prediction scheme of Glegg.[3] Their results showed that the turbulence of an undisturbed vortex is insufficient to account for most of the BWI noise generated.

Most previous work on perpendicular interactions has been concerned with effects on the aerodynamic characteristics of the blade rather than on the vortex itself. Kalkhoran et al[4]. examined the influence of a trailing vortex on a rectangular NACA 0012 section blade at zero angle of attack for Mach numbers between 0.7 and 0.8 and blade-vortex separations Δ of 0.3–0.1 chord lengths c. The vortex was found to alter the pressure distribution on the blade especially upstream of its maximum thickness; this effect increases with reduction in Δ. The vortex also drifted in the spanwise direction as it passed over the blade, under the influence of its image in the blade surface. Phillipe and Armand[5] studied the influence of a trailing vortex on the integrated lift and drag of a rectangular NACA 0012 blade at a Mach number of 0.6 for constant Δ. The vortex was found to reduce the blade lift and to increase drag by as much as 40% in the presence of the vortex. Seath and Wilson[6] studied interactions with a rectangular NACA 64A015 blade at zero angle of attack at a chord Reynolds number of 417,000. They observed significant changes in the pressure distribution on the blade in the vicinity of the vortex as well as the spanwise drift of the vortex over the blade surface. Flow visualizations were also performed which show three-dimensional separation and reattachment lines induced by the nearby vortex. Müller[7] used laser Doppler anemometry to examine the mean flow structure immediately downstream of a blade-vortex interaction for a chord Reynolds number of 100,000. He used a blade with varying twist angle to simulate the lift distribution on a helicopter blade with the trailing vortex passing on the pressure side

Received Feb. 14, 1994; revision received Jan. 4, 1995; accepted for publication Feb. 16, 1995.

*Graduate Student, Department of Aerospace and Ocean Engineering, 215 Randolph Hall.
†Associate Professor, Department of Aerospace and Ocean Engineering, 215 Randolph Hall. Senior Member AIAA.
‡Graduate Student, Department of Aerospace and Ocean Engineering, 215 Randolph Hall. Student Member AIAA.
§Professor, Center of Acoustics and Vibration, Department of Ocean Engineering, NW 28th Street. Member AIAA.

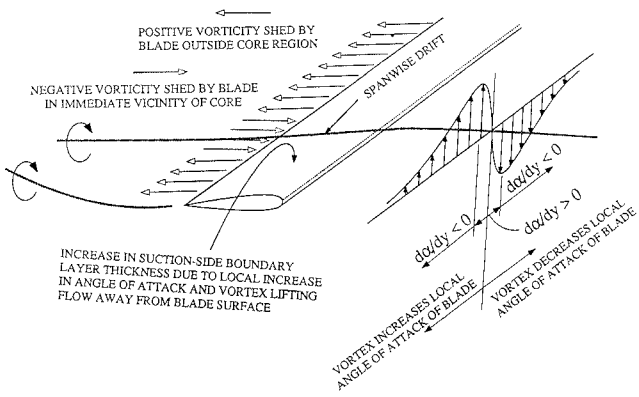

Fig. 1 Primary features of a perpendicular blade-vortex interaction, suction-side passage.

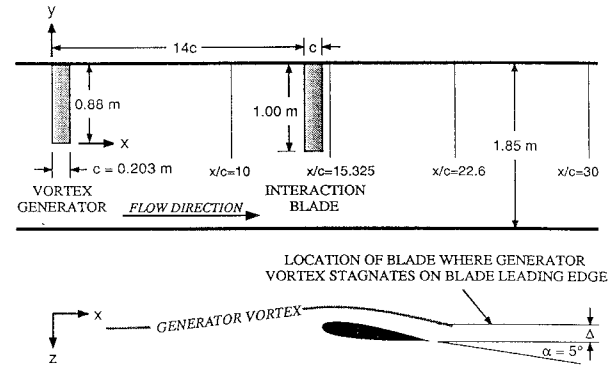

Fig. 2 Wind-tunnel schematic and coordinate system.

of the blade near the tip. Based on his measurements and theoretical considerations, he postulates that the disturbance caused by the vortex on the blade lift distribution causes the local shedding of a midspan vortex with a strength of one-quarter to one-third of that of the blade tip vortex. Ham[8] measured surface pressure distributions on a blade as the streamwise vortex oscillated periodically across its leading edge. Ham concluded that the disturbance to the blade pressure distribution cannot exceed a certain peak value, beyond which the flow under the vortex stalls. He argues that this peak value is dependent on the two-thirds power of the vortex circulation and is largely independent of blade pitch or yaw angle.

Beginning with the cited results one can infer some major features of flow over a blade in the presence of a streamwise vortex (Fig. 1). Velocities associated with the vortex change the local angle of attack α of the blade: increasing it outboard of the vortex center and decreasing it inboard. These changes have a strong influence on the blade boundary layer and wake. Outboard of the vortex center the thickness of the suction-side boundary layer and the resulting wake are increased by the additional angle of attack. If the vortex is sufficiently strong, or the encounter sufficiently close, a local separation may be induced on the suction surface. Conversely, inboard of the vortex center the boundary layer and the wake thickness will be decreased by the presence of the vortex. Since the vortex produces a change in angle of attack along the blade span, it also induces the formation of streamwise vorticity in the blade boundary layers, which is shed into the wake. Inboard and outboard of the core $\partial\alpha/\partial y$ is positive and positive vorticity is shed. In the immediate vicinity of the core, negative vorticity is shed. As the vortex passes over the blade it drifts under the influence of its image: inboard for pressure-side passage, outboard for suction-side passage (depicted in Fig. 1). Downstream of the blade it is expected that the vortex will interact with both the blade wake and the blade tip vortex.

The present study—unlike those outlined earlier—is aimed at understanding the development of the vortex downstream of the blade. Flow visualizations as well as detailed velocity and turbulence measurements have been made on a model flow. The results have been incorporated into the theoretical noise prediction scheme of Glegg.[3] The purpose of the present paper is to describe and discuss the experimental results.

Apparatus and Instrumentation

Apparatus and instrumentation are described in detail by Devenport et al.[9] Only brief descriptions of these items are described next.

Wind Tunnel

Experiments were performed in the Virginia Tech Stability Wind Tunnel. It is a closed-circuit tunnel powered by a 600-hp axial fan. The test section has a square cross section, 1.83 × 1.83 × 7.33 m. Flow in the empty test section is closely uniform with a turbulence intensity of less than 0.05%. A slight favorable pressure gradient exists along the test section due to boundary-layer growth, which causes some convergence of the streamlines. Flow angles are small near the middle of the section but increase to about 2 deg near the walls.[10]

Blades

Untwisted NACA 0012 blades were used: one to generate the vortex and the other to interact with it. Both had a rectangular planform of 0.203-m chord and blunt wing tips. Boundary-layer trips were placed on both blades. These consisted of 0.5-mm-diam glass beads glued in a random pattern along the entire span between the 20% and 40% chord locations. The vortex generator blade was mounted vertically as a half-wing at the center of the upper wall of the test section entrance with 0.879 m protruding into the flow (Fig. 2). The interaction blade was mounted similarly, 14 c downstream with an effective half-span of 1.003 m, the longer span ensuring a blade-vortex interaction approximately 0.85 c from the blade tip. The angle of attack of both wings was set at 5 deg measured according to the right-hand rule for the negative y axis shown in Fig. 2. The position of the interaction blade could be varied laterally to change the blade-vortex separation distance.

Hot-Wire Anemometry

An Auspex Corp. miniature four-sensor hot-wire probe, type AVOP-4-100, was used to make three component velocity measurements. The probe consists of two orthogonal X-wire arrays with a total measurement volume of 0.4 mm^3. The sensors were operated using four Dantec 56C17/56C01 anemometer units balanced to give a frequency response of better than 20 kHz. The output voltages from the anemometer bridges were recorded by an IBM AT compatible computer using an Analogic 12 bit HSDAS-12 analog-to-digital converter. Sensor wire angles were determined by pitching and yawing the probe in the uniform potential core of a jet. The probe was calibrated frequently in the freestream by using King's law to correlate the wire output voltages with the cooling velocities. The absolute flow direction at the calibration location was determined in advance using a seven-hole yaw probe. Hot-wire signals were corrected for temperature changes using the method of Bearman.[11]

Flow Visualization

Flow visualizations were performed by seeding the flow with helium-filled soap bubbles produced with a Sage Action Inc. model 5 generator. Being lighter than air, the bubbles centrifuge into the vortex core, marking it clearly. Still photographs and videos were used to record the visualizations.

Results and Discussion

The wind-tunnel fixed coordinate system (Fig. 2) centered at the leading edge of the vortex generator tip will be used in presenting results. In this system, the leading edge of the interaction blade is at $x/c = 14$ and its tip is at $y/c = -0.613$. Measurements were made for several lateral z positions of the interaction blade measured in terms of the blade-vortex separation distance Δ, defined in Fig. 2. Zero Δ corresponds to the blade position where the streamline marking the vortex center stagnates upon the blade leading edge. Δ is negative when the vortex passes on the pressure side of the blade and positive when it passes on the suction side.

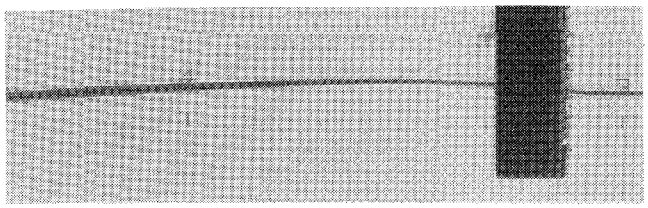

Fig. 3 Helium bubble flow visualization, $\Delta/c = -0.0625$, pressure-side passage; flow is from right to left, photographic negative shown.

Flow Visualizations

A large number of flow visualizations were performed over a broad range of conditions, all of which are described by Rife and Devenport.[12] For the conditions matching the velocity measurements, a range of phenomena were observed depending on Δ.

For Δ greater than a few percent chord the vortex is deflected as it passes the interaction blade under the influence of its image in the blade. This deflection is inboard for pressure side passage (shown in Fig. 3) and outboard for suction side passage. Initially the interaction appears to have no influence on the core. Downstream of the interaction blade, however, the vortex core (at least as it is marked by the bubbles) grows more rapidly and becomes more turbulent. It also interacts with the tip vortex shed by the interaction blade, the two rotating slowly about each other with distance downstream (Fig. 3). The magnitude of these effects increased with reduction in Δ.

For Δ near zero ($|\Delta| < 0.0625\,c$), the form of the interaction is quite different. The vortex appears to split into two filaments at the leading edge of the blade: one passing on the pressure side and the other on the suction side. Downstream of the interaction blade the filaments rapidly loose their coherence, becoming indistinguishable from the surrounding turbulent flow.

Velocity Measurements

Measurements in the y–z plane were made 4 chord lengths upstream of the blade leading edge ($x/c = 10$) and 0.325, 7.6, and 15 chord lengths downstream of its trailing edge ($x/c = 15.325$, 22.6, and 30) for blade-vortex separations (Δ/c) of ± 0.125, ± 0.0625, and 0. All measurements were made at a chord Reynolds number of 260,000 corresponding to a freestream velocity U_{ref} of about 20 m/s. The uncertainty in the velocity measurements is estimated to be: ± 0.015 for U/U_{ref}, ± 0.025 for V/U_{ref} and W/U_{ref}, $\pm 2.9 \times 10^{-5}$ for k/U_{ref}^2 in the core region, and $\pm 1.4 \times 10^{-5}$ for k/U_{ref}^2 in the wake region. Because of the volume of data only a representative sample is presented here. An unabridged presentation of the measurements is given by Devenport et al.[9]

Undisturbed Vortex

A z-wise mean velocity profile through the core at $x/c = 10$ (4 chordlengths upstream of the blade leading edge) is shown in Fig. 4. The axial (U) velocity profile is approximately Gaussian in the vicinity of the core and shows a peak deficit of some 15% U_{ref}. The tangential (V) velocity profile is closely antisymmetric about the core center. It shows a peak tangential velocity at the core edge of 27.2% U_{ref}, a core radius of 3.8% c and a steep velocity gradient at the core center. Assuming axisymmetry, the core circulation is 27% Γ_0. Outside the core the tangential velocity profile compares well with a Betz's theory calculation[13] based on the theoretical lift distribution of the vortex generator. The differences that do exist are probably due to nonaxisymmetry of the flow.

This nonaxisymmetry is clearly visible in the contours of turbulence kinetic energy (k/U_{ref}^2) (Fig. 5) which show the vortex generator wake is wound in a loose spiral. Far from the core the structure of the wake is indistinguishable from that of a two-dimensional wake. As the core is approached along the spiral, however, significant three-dimensional effects are seen. First, peak turbulence levels rise, reaching a maximum of 0.0005 at $(y/c, z/c) = (0.3, 0.35)$. They then fall as the wake wraps around the core reaching 0.00025 at $(0.15, -0.15)$. The decrease in turbulence levels may be due to the straining of the wake in the rotational velocity field of the vortex, which probably inhibits the formation and or development of large-scale coherent structures.

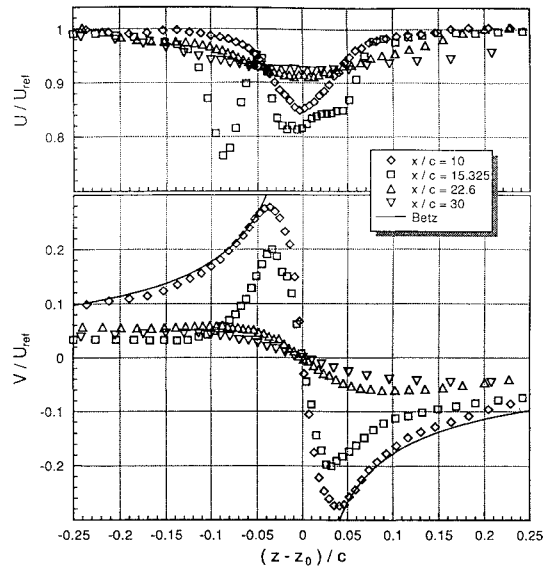

Fig. 4 Mean z-wise velocity profile along the lines: $y/c = 0.18$ at $x/c = 10$, $y/c = 0.33$ at $x/c = 15.325$, $y/c = 0.11$ at $x/c = 22.6$, and $y/c = -0.18$ at $x/c = 30$.

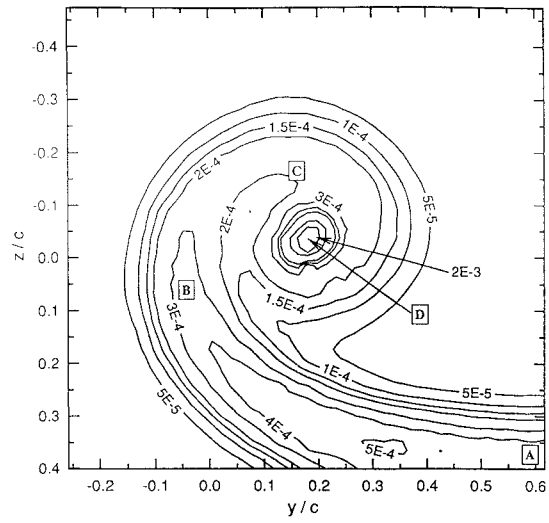

Fig. 5 Contours of turbulent kinetic energy (k/U_{ref}^2) at $x/c = 10$.

This hypothesis appears supported by the summed V and W velocity autospectra $G_{vv} + G_{ww}$ shown in Fig. 6; the sum is used to eliminate the need for a coordinate system rotation along the wake. (Note that these spectra are samples from a much more detailed set.) The spectrum in the far wake (curve A measured at location A in Fig. 5) is very similar to a standard two-dimensional wake spectrum as presented by Antonia and Britz.[14] The peak near $fc/U_{\text{ref}} = 3.5$ presumably marks the passage frequency of large-scale structures. Assuming Taylor's hypothesis this indicates a structure spacing of about $0.3c$, a distance approximately equal to the wake thickness at this location. At higher frequencies this spectrum shows the expected inertial subrange ($-5/3$ slope) and then a rolloff toward the dissipation range (-7 slope). Moving along the 180-deg bend in the wake toward the core (points B and C), a loss of low-frequency ($fc/U_{\text{ref}} < 10$) energy flattens the peak at $fc/U_{\text{ref}} = 3.5$ suggesting that the larger scale structures are weaker or less coherent here. Surprisingly, at frequencies above $fc/U_{\text{ref}} = 10$, spectral levels remain almost unaltered. Thus, the suppression of low-frequency motions does not influence the amplitude of high-frequency motions as might be expected through the energy cascade.

Moving into the core, measured turbulence kinetic energy levels (Fig. 5) greatly increase. This is a consequence of small lateral wandering motions of the core rather than a sign of increased turbulent activity. Velocity fluctuations in the core are consistent

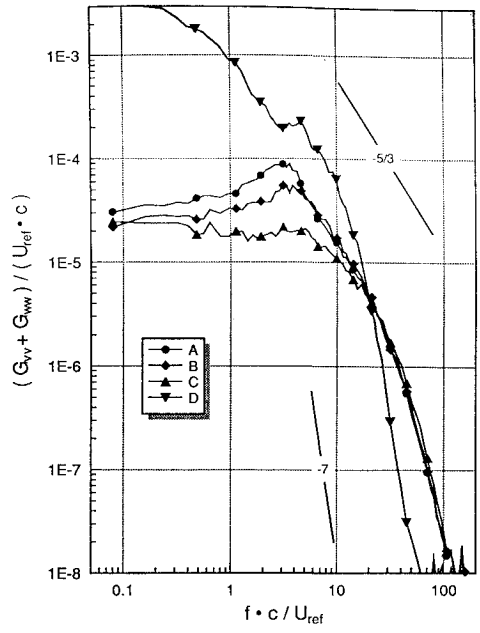

Fig. 6 Velocity autospectra at $x/c = 10$, legend refers to measurement locations shown in Fig. 5.

with wandering motions of an rms amplitude of only $0.005\,c$ (7% core diameter) given the steep tangential velocity gradient here. The motions are visible at the low-frequency end ($fc/U_{\text{ref}} < 2$) of core spectra (e.g., point D) where energy levels are greatly elevated. If these low-frequency contributions due to wandering did not exist, it appears that turbulence levels would continue to decrease as the core center is approached. Moving from the wake into the core, spectral levels at high frequencies fall and the inertial subrange disappears. At frequencies above $fc/U_{\text{ref}} = 35$ spectral levels are only about 10% of those seen on the wake centerline far from the core. More extensive undisturbed vortex measurements by Devenport et al.[15] show this to be indicative of a laminar core flow.

Pressure Side Passage, $\Delta/c = -0.0625$

Measurements were made at $x/c = 15.325$, 22.6, and 30. Contours of turbulent kinetic energy immediately downstream of the blade at $x/c = 15.325$ (Fig. 7) show the interaction blade to have cut the spiral wake of the vortex generator in two. The generator core is centered near (0.33, 0.02) just to the pressure side of the blade wake and $0.94\,c$ inboard of the blade tip. The difference in core y position at $x/c = 10$ and 15.325 indicates a spanwise drift of the core during its interaction with the blade of some $0.09\,c$ inboard. Also, turbulence levels in the spiral wake have decreased over the $5.325\,c$ downstream which it has traveled. Otherwise, the structure of this wake appears to be similar to that at $x/c = 10$ with turbulence levels still decreasing along the spiral as the core is approached.

The blade wake at $x/c = 15.325$ appears to be thicker and more turbulent outboard than inboard of the vortex core. This thickening is due to the effects of the vortex on the local angle of attack of the blade α. Judging from the tangential velocity profile at $x/c = 10$, the local angle of attack on the blade could change by as much as ± 15 deg near the generator core and $+2$ deg at the blade tip. Mean streamwise vorticity contours (Fig. 8) show that both inboard and outboard of the generator core, positive streamwise vorticity is shed from the blade into its wake. In the vicinity of the core, the expected region of negative mean vorticity is also visible. This appears in a highly distorted part of the wake. Turbulence stress levels and turbulence kinetic energy production (not shown) are elevated in this region indicating increased mixing (see Devenport et al.[2]). The peak negative mean vorticity is about 25% of the peak positive vorticity of the generator core.

A tangential mean-velocity profile through the generator core center (Fig. 4) provides evidence that the region of negative mean vorticity is not just adjacent to the core but is being ingested by

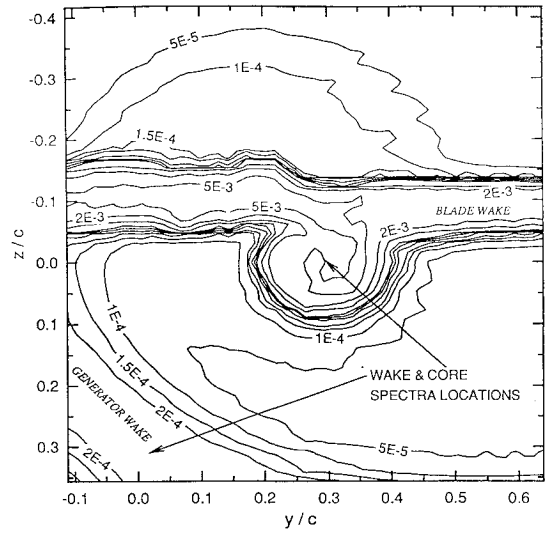

Fig. 7 Contours of turbulent kinetic energy (k/U_{ref}^2) at $x/c = 15.325$, $\Delta/c = -0.0625$.

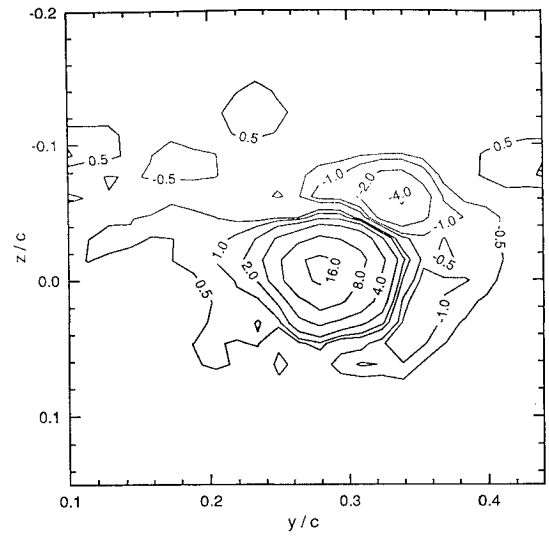

Fig. 8 Contours of mean streamwise vorticity ($\omega_x c/U_{\text{ref}}$) at $x/c = 15.325$, $\Delta/c = -0.0625$.

it. The profile shows a reduced core radius of 3.1% c and a peak tangential velocity of 19.4% U_{ref}, implying a core circulation of only 15.7% Γ_0 (only about 3/5 the value at $x/c = 10$). Many previous authors (e.g., Shabaka et al.[16]) have observed the generation of negative vorticity during vortex/boundary-layer interaction and the consequent weakening of the core. The decrease in core circulation obviously eliminates any correlation between the tangential velocity field and Betz's theory as shown in Fig. 4.

The axial mean-velocity profile through the generator core shows both the deficit due to the vortex (centered near $z = z_0$) and that due to the blade wake [centered at about $(z - z_0)/c = -0.085$]. The peak deficit due to the vortex core has increased by 3.4% U_{ref} from upstream at $x/c = 10$, perhaps partly due to the ingestion of blade-wake fluid and the effects of streamwise pressure gradients imposed by the wing.

The subsequent streamwise development of this flow is shown by the turbulent kinetic energy contours measured at x/c of 22.6 and 30 (Fig. 9 and 10). These contours include the tip vortex of the interaction blade near the upper left-hand corner of the figures. The generator vortex core (identified by a local maximum in k approximately centered in the figures) appears well embedded in the blade wake. The generator wake can also be seen at these locations, but the high turbulence levels of the superimposed blade wake mask much of the loose spiral seen at $x/c = 10$ and 15.325.

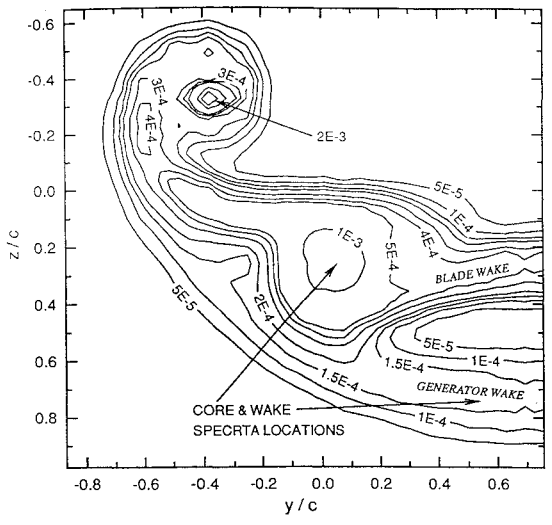

Fig. 9 Contours of turbulent kinetic energy (k/U_{ref}^2) at $x/c = 22.6$, $\Delta/c = -0.0625$.

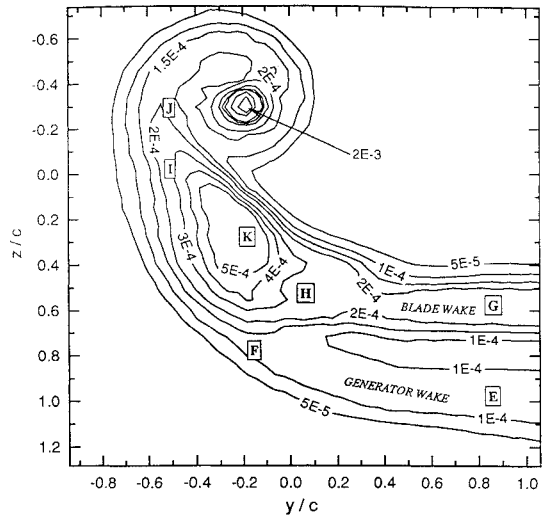

Fig. 10 Contours of turbulent kinetic energy (k/U_{ref}^2) at $x/c = 30$, $\Delta/c = -0.0625$.

Comparing Figs. 5, 7, 9, and 10 and noting the changes in scale, one sees that the interaction produces a region of turbulent flow much greater cross section and intensity than that presented by the undisturbed vortex. It also causes the formation and dramatic enlargement of a region of highly turbulent flow in the vicinity of the core. For example, the area of normalized turbulence kinetic energy (k/U_{ref}^2) turbulence levels above 0.0005 at $x/c = 30$ is about 10 times that at $x/c = 10$. Note that streamwise vorticity contours show the negative region adjacent to the core to be absent at $x/c = 22.6$ and 30, having been absorbed into the rapidly expanding core.

Figure 4 compares mean velocity profiles through the generator core at these locations with those measured upstream. Figure 11 summarizes the development of these profiles in terms of core parameters. Note that tangential velocity profiles measured at $x/c = 22.6$ and 30 contained a substantial contribution from the tip vortex of the interaction blade (which we have subtracted). This contribution was estimated using Betz's theory (see Devenport et al.[9]). These figures show the rapid growth of the core and decay of its tangential and axial mean velocity fields that result from the interaction. The core radius at $x/c = 30$ is five times greater than at $x/c = 15.325$, whereas the peak tangential velocity decreases from 19.4% U_{ref} to 4.5% U_{ref} and the axial velocity deficit falls from 18.4% U_{ref} to 6% U_{ref}. Despite these dramatic changes, the core circulation remains almost constant at about 18% Γ_0 after the interaction.

Summed V and W velocity autospectra measured throughout the body of the blade and vortex generator wakes at $x/c = 30$, shown in

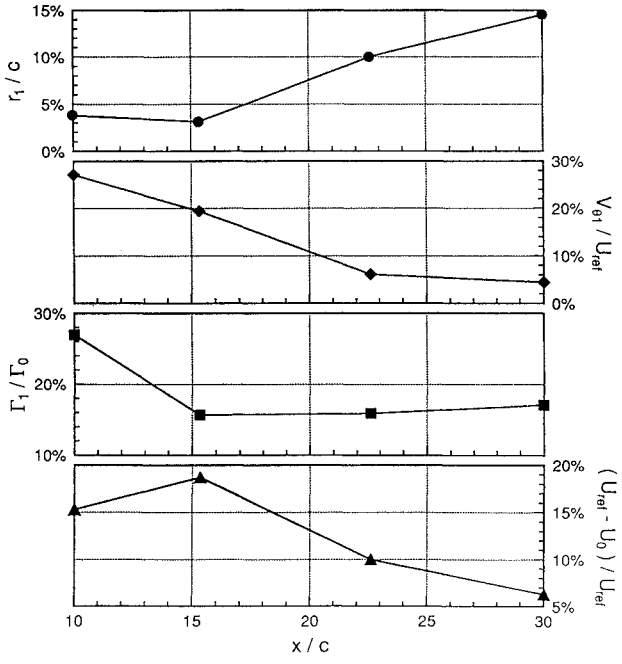

Fig. 11 Generator vortex core parameters as a function of x/c for $\Delta/c = -0.0625$.

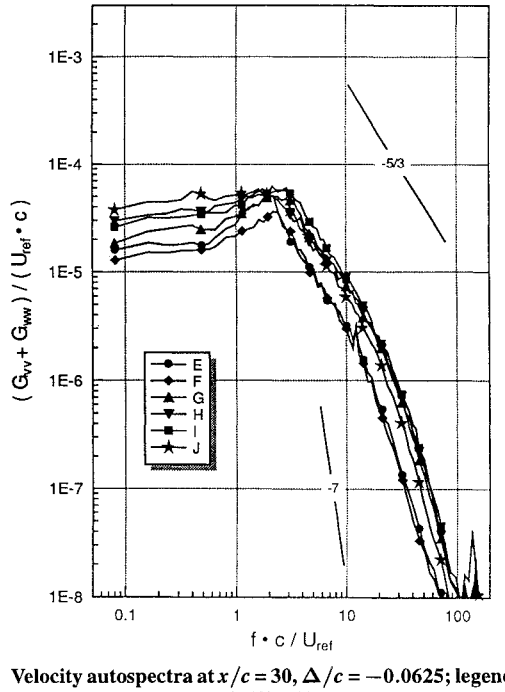

Fig. 12 Velocity autospectra at $x/c = 30$, $\Delta/c = -0.0625$; legend refers to measurement locations shown in Fig. 10.

Fig. 12, may be compared with those measured in the undisturbed generator wake at $x/c = 10$ (Fig. 5). Spectral levels and characteristic frequencies in the generator wake (points E and F) have decreased with downstream distance much as they would if the wake were growing in isolation, and the basic form of the spectrum has not been changed much by the interaction. The form of the spectrum in most parts of the blade wake (points G–J) is also very similar, though spectral levels and characteristic frequencies are higher because of the shorter distance over which this wake has grown.

Although there is little qualitative effect of the interaction on the turbulence spectrum outside the generator core, the same cannot be said inside the core. Figure 13 shows autospectra measured near the core center as a function of x. Clearly the interaction produces a significant and almost immediate change. At all locations downstream of the interaction the spectra show a clear $-5/3$ region, and

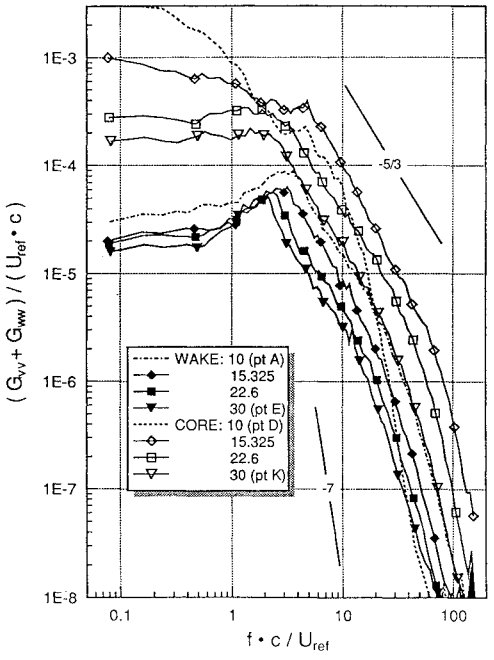

Fig. 13 Velocity autospectra at x/c = 15.325, 22.6, and 30 (Δ/c = −0.0625), legend refers to measurement locations shown in Figs. 7, 9, and 10, respectively.

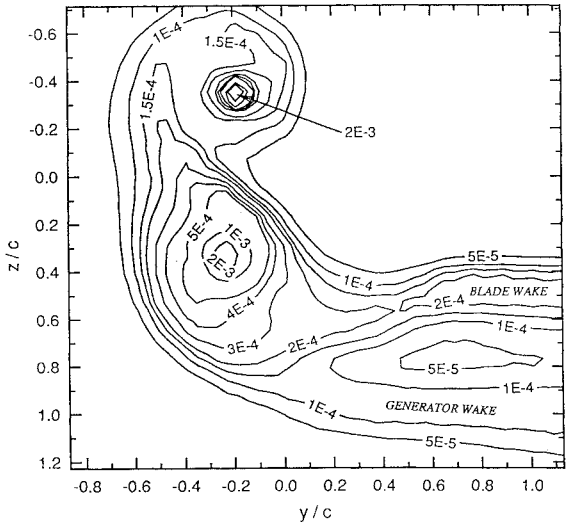

Fig. 14 Contours of turbulent kinetic energy (k/U_{ref}^2) at x/c = 30, Δ/c = −0.125.

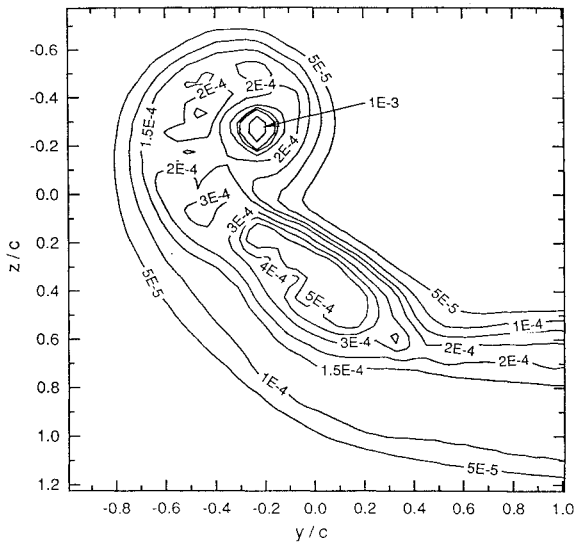

Fig. 15 Contours of turbulent kinetic energy (k/U_{ref}^2) at x/c = 30, Δ/c = 0.

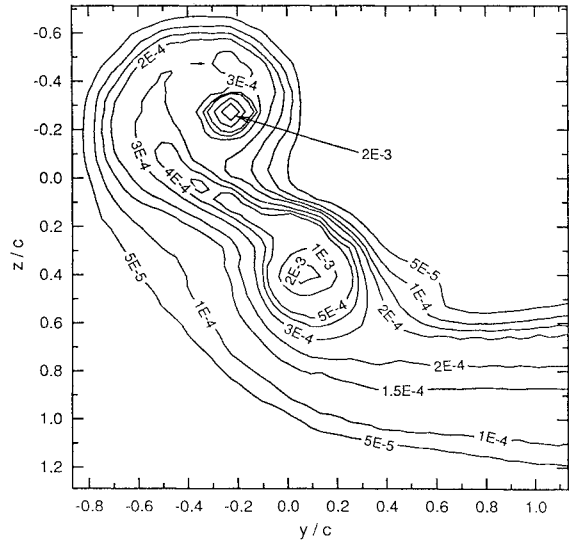

Fig. 16 Contours of turbulent kinetic energy (k/U_{ref}^2) at x/c = 30, Δ/c = 0.0625.

the spectral shape at frequencies above $fc/U_{ref} = 5$ is very similar to the wake spectra (examples of which are included in this figure). Spectral levels at frequencies above $fc/U_{ref} = 35$ within the primary core after interaction are more than 10 times as great as peak levels in the wake far from the core; unlike data at $x/c = 10$ where core levels were only 10% of the wake levels at these frequencies. The implication here is that, following the blade vortex interaction, flow in the core becomes highly turbulent, consistent with the rapid growth and decay of the core mean-flow structure seen here.

Other Blade-Vortex Separations

Measurements were to determine the effects of blade-vortex separation on the flow structure at $x/c = 30$. Blade-vortex separations (Δ/c) of −0.125, 0, 0.0625, and 0.125 were also studied. Whereas these measurements (Figs. 14–17) show all of the geometrical changes one would expect to see—variations in the relative locations of the blade and vortex generator cores and corresponding changes in the positions and shapes of the wakes—they reveal few qualitative changes in the underlying turbulence structure. For all Δ, turbulence kinetic energy contours show the vortex generator core to be marked by an enlarged region of highly turbulent flow embedded in the blade wake. For $\Delta = 0$, the disruption to the core is so complete (presumably as a consequence of it splitting on the blade leading edge) that it was not possible to define its exact center and extent from mean-velocity measurements. For all Δ, spectra measured in the core (or its remnant) and surrounding wakes are of similar shape and level to those presented for $\Delta/c = -0.0625$, and turbulence levels in the core are higher than levels in the surrounding wakes at all frequencies.

Quantitatively, the variation in Δ produces large variations in core radius and peak tangential velocity (Fig. 18). For both separation distances ($|\Delta/c| = 0.125$ and 0.0625), pressure-side passage produces a greater disruption to the core resulting in a larger core size and lower peak tangential velocity and axial velocity deficit at $x/c = 30$. As might be expected, a smaller separation distance causes greater disruption to the core; halving the separation distance roughly causes a doubling of the core radius at $x/c = 30$. Furthermore, variation in Δ produces almost the same proportionate change in peak tangential velocity and axial velocity deficit. Surprisingly, core circulation at $x/c = 30$ is roughly constant (~17% Γ_0) for $\Delta/c = -0.125$, −0.0625 and 0.0625; but for $\Delta/c = -0.125$ it is significantly greater (23% Γ_0). The jump in core circulation hints at the possibility of an on–off type of effect, depending on Δ.

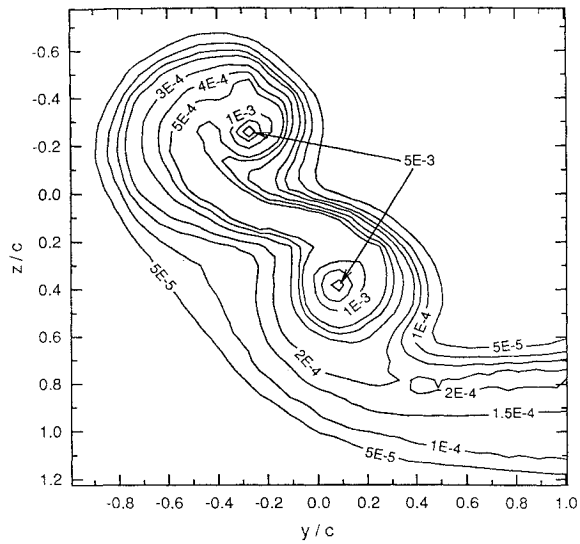

Fig. 17 Contours of turbulent kinetic energy (k/U_{ref}^2) at $x/c = 30$, $\Delta/c = 0.125$.

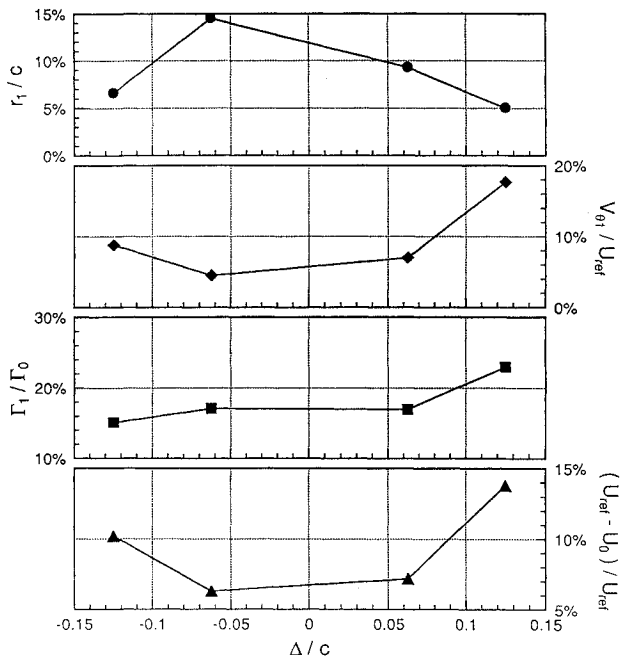

Fig. 18 Generator core parameters as a function of Δ/c for $x/c = 30$.

One intriguing effect of Δ is on the peak turbulence levels in the highly curved section of blade wake that joins the generator and blade tip vortex cores. Peak levels increase as Δ becomes more positive. Consider, for example, turbulence kinetic energy in the most elevated (i.e., most negative z) section of the blade wake. For $\Delta/c = -0.125$ (Fig. 14) k/U_{ref}^2 reaches a peak value of about 1.5×10^{-4} here. For $\Delta/c = 0.125$ (Fig. 17) the peak value is at least three times greater. Effects of similar magnitude are visible along this entire section of wake and in the blade tip vortex core. A possible explanation of this lies in the effect of the generator vortex on the blade boundary layer. However, the influence of the blade tip vortex on the turbulence structure in this region is also probably strong. Although it was possible with some certainty to subtract out the effects of the blade tip vortex from the mean velocity profiles, its effects on the turbulence field are not as easy to comprehend. Thus, further experiments are planned with an interaction blade which spans the entire tunnel, thus eliminating the difficulties presented by the blade tip vortex.

Concluding Remarks

The effects of placing a lifting blade in the path of a trailing vortex have been studied through detailed velocity measurements and flow visualizations for blade-vortex separations from −0.125 to 0.125 chords.

Upstream of the blade, the vortex consists of a turbulent wake wound into a spiral surrounding a laminar core; high-frequency velocity fluctuations in the core are an order of magnitude less than in the wake. The core contains 27% of the total circulation. Outside of the core, the tangential velocity field is closely described by Betz's theory.

The passage of the vortex over the blade significantly alters the blade circulation distribution, causing negative vorticity to be shed into its wake. This vorticity rapidly becomes entrained into the vortex core almost halving its circulation and also eliminating any correlation between the tangential velocity field and Betz's theory.

The interaction with the blade and its turbulent wake stimulates a large increase in the core growth rate and the decay rate of its tangential and axial velocity fields. Also, high-frequency velocity fluctuation levels in the core greatly increase and velocity autospectra measured here show an inertial subrange. These effects suggest that the core flow has become fully turbulent.

This large turbulent vortex core winds the blade wake and its own spiral wake into a turbulent flow of much larger cross section and intensity than that presented by the undisturbed vortex. Throughout this flow, velocity autospectra have a form qualitatively similar to that of a two-dimensional wake.

Varying the blade vortex separation over the range studied does not qualitatively change the effects of the interaction. Quantitatively, lower blade-vortex separations produce a more rapid decay of the vortex core downstream of the blade; the effects tend to be greater when the vortex passes to the pressure side of the blade. Interestingly, the loss in core circulation produced by the interaction is almost constant for a range of blade-vortex separations.

These conclusions have important implications for helicopter noise prediction when several blades interact with the same tip vortex. If the first interaction is perpendicular and sufficiently close (as will often occur in level flight and mild climb conditions), then the preceding results suggest that it will produce a large region of turbulent flow in the vicinity of the vortex, a substantial enlargement in the core diameter, and modification of the tangential velocity field. The first of these effects is likely to substantially increase the broadband BWI noise generated by subsequent perpendicular interactions. The last two will have a significant effect on noise generated by subsequent parallel interactions which cause impulsive BVI noise. Providing more detailed empirical information on the functional variation of core size and velocity distribution in terms of the parameters of the blade vortex interaction is a priority of future work.

The complete set of time-averaged data may be accessed on the World Wide Web at http://www.aoe.vt.edu/flowdata.html.

Acknowledgments

The authors would like to thank NASA Langley, in particular, Tom Brooks and Mike Marcolini, for their support under Grant NAG-1-1119. The assistance of Mark Engel, Chris Shively, and Lee Fugelstad in taking many of the measurements is also gratefully acknowledged.

References

[1]Brooks, T. F., and Martin, R. M., "Results of the 1986 NASA/FAA/DFVLR Main Rotor Test Entry in the German-Dutch Wind Tunnel (DNW)," NASA TM 100507, 1987.

[2]Devenport, W. J., Glegg, S. A. L., and Sharma, G., "Turbulence Measurements in Trailing Vortices for B.W.I. Noise Prediction," Rept. to NASA Langley, Grant NAG-1-1119, 1992.

[3]Glegg, S. A. L., "The Prediction of Blade-Wake Interaction Noise Based on a Turbulent Vortex Model," AIAA Paper 89-1134, April 1989.

[4]Kalkhoran, I. M., Wilson, D. R., and Seath, D. D., "Experimental Investigation of the Perpendicular Rotor Blade-Vortex Interaction at Transonic Speeds," *AIAA Journal*, Vol. 30, No. 3, 1992, pp. 747–755.

[5]Phillipe, J. J., and Armand, C., "ONERA Aerodynamic Research on Helicopters," *Rotorcraft Design*, AGARD CP-223, Jan. 1978.

[6]Seath, D. D., and Wilson, D. R., "Vortex-Airfoil Interaction Tests," AIAA Paper 86-0354, Jan. 1986.

[7]Müller, R. G. H., "Special Vorticies at a Helicopter Rotor Blade," *Journal of the American Helicopter Society*, Vol. 35, No. 4, 1990, pp. 16–22.

[8]Ham, N. D., "Some Conclusions From an Investigation of Blade Vortex Interaction," *Journal of the American Helicopter Society*, Vol. 20, No. 4, 1975, pp. 26–31.

[9]Devenport, W. J., Glegg, S. A. L., Wittmer, K. S., and Rife, M. C., "Perpendicular Blade Vortex Interaction and its Implications for Helicopter Noise Prediction," Virginia Polytechnic Inst. and State Univ., Rept. VPI-AOE-214, Blacksburg, VA, 1994.

[10]Choi, K., and Simpson, R. L., "Some Mean-Velocity, Turbulence, and Unsteadiness Characteristics of the VPI&SU Stability Wind Tunnel," Virginia Polytechnic Inst. and State Univ., Rept. VPI-AOE-161, Blacksburg, VA, 1987.

[11]Bearman, P. W., "Corrections for the Effect of Ambient Temperature Drift on Hot-Wire Measurements in Incompressible Flow," *DISA Information*, No. 11, May 1971, pp. 25–30.

[12]Rife, M. C., and Devenport, W. J., "Flow Visualizations of Perpendicular Blade Vortex Interactions, Virginia Polytechnic Inst. and State Univ., Rept. VPI-AOE-197, Blacksburg, VA, 1993.

[13]Donaldson, C. du P., and Bilanin, A. J., "Vortex Wakes of Conventional Aircraft," AGARD AG 204, 1975.

[14]Antonia, R. A., and Britz, D., "Phase Averaging in the Turbulent Far-Wake," *Experiments in Fluids*, 1989, Vol. 7, pp. 138–142.

[15]Devenport, W. J., Rife, M. C., Liapis, S. I., and Follin, G. J., "Turbulence Structure and Scaling in Trailing Vortices," AIAA Paper 95-0588, 1995.

[16]Shabaka, I. M. A., Mehta, R. D., and Bradshaw, P., "Longitudinal Vorticies Embedded in Turbulent Boundary Layers. Part 1. Single Vortex," *Journal of Fluid Mechanics*, Vol. 155, 1985, p. 37.